nature portfolio

https://doi.org/10.1038/s41586-021-03857-w

Supplementary information

Structure of *Geobacter* pili reveals secretory rather than nanowire behaviour

In the format provided by the authors and unedited

Supplementary Information (SI)

Structure of *Geobacter* pili reveals secretory rather than nanowire behaviour

Yangqi Gu[1,2,5], Vishok Srikanth[1,3,5], Aldo I. Salazar-Morales[1,3], Ruchi Jain[1,3], J. Patrick O'Brien[1,3], Sophia M. Yi[1,3], Rajesh K. Soni[4], Fadel A. Samatey[1,3], Sibel Ebru Yalcin[1,3], and Nikhil S. Malvankar[1,3]

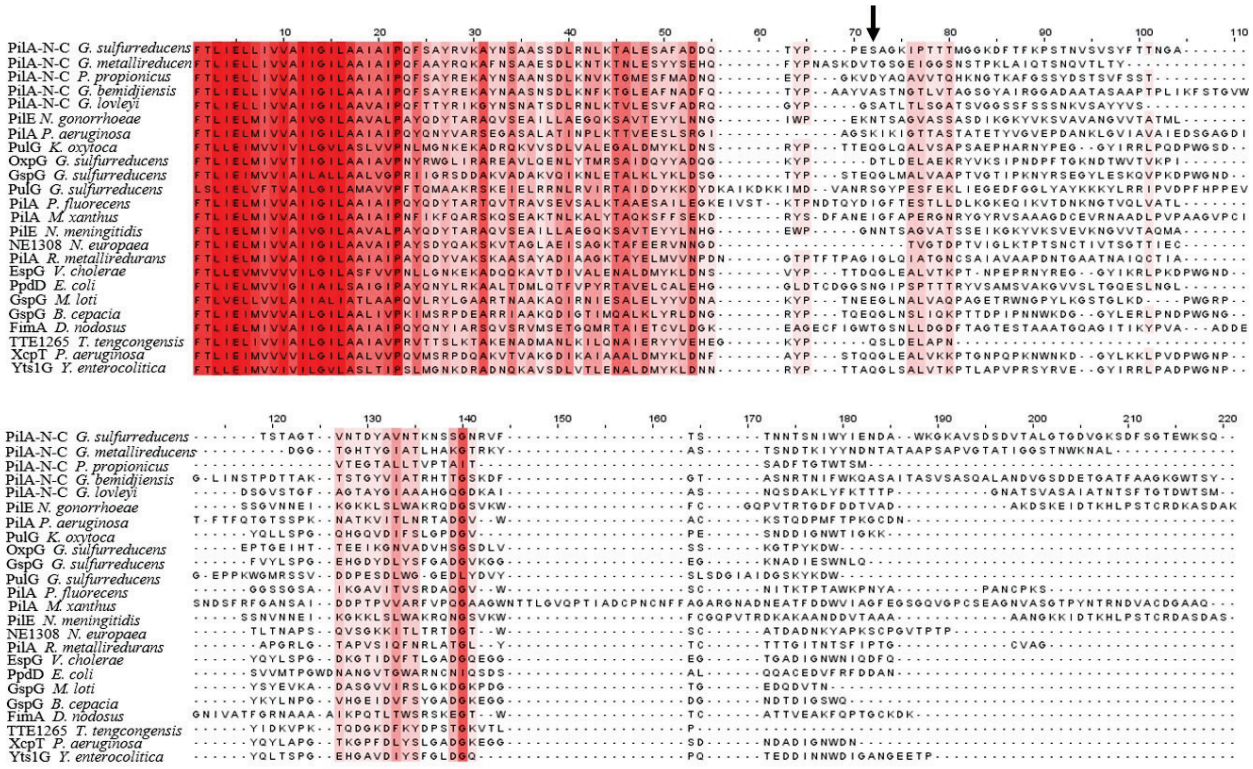

Supplementary Data Figure 1a. Amino acid sequence alignment of the T4P-like proteins from different species showed that N-terminal are highly conserved, while the C-terminal is divergent. Sequence conservation is rendered in red, and a darker colour represents a higher conservation score. For *Geobacter*-related species, PilA-N and PilA-C sequences were fused together for comparison. Black arrow shows the location where the PilA-N sequence ends. This sequence alignment was used to construct the phylogenetic tree shown in Fig. 1b.

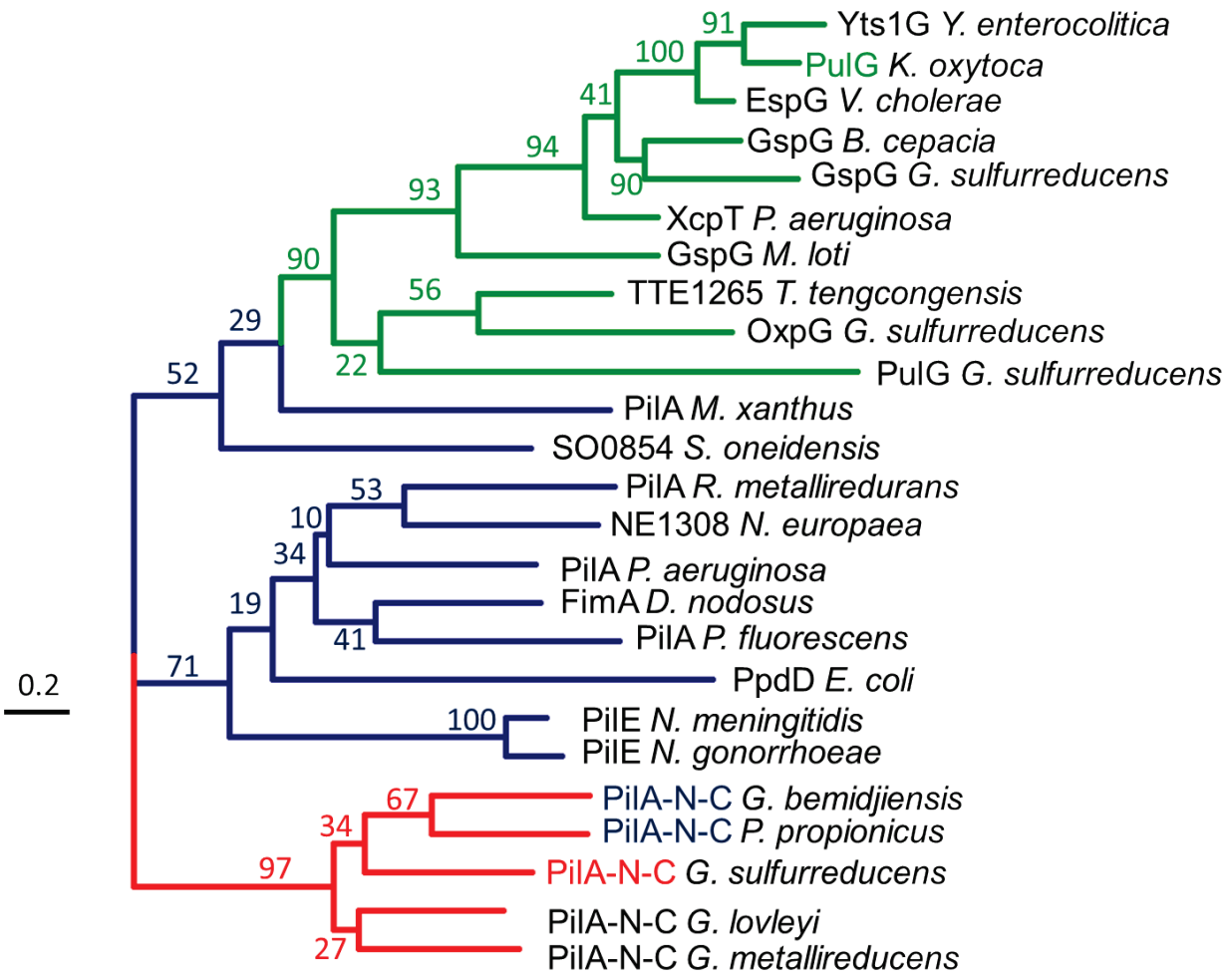

Supplementary Data Figure 1b. Phylogenetic analysis of pilin amino acid sequence alignment of the T4P (blue) and T2SS pseudopili (green) from different species. For *Geobacter*-related species, PilA-N and PilA-C sequences were fused together for comparison (shown in red). Numbers represent bootstrap values for each branch.

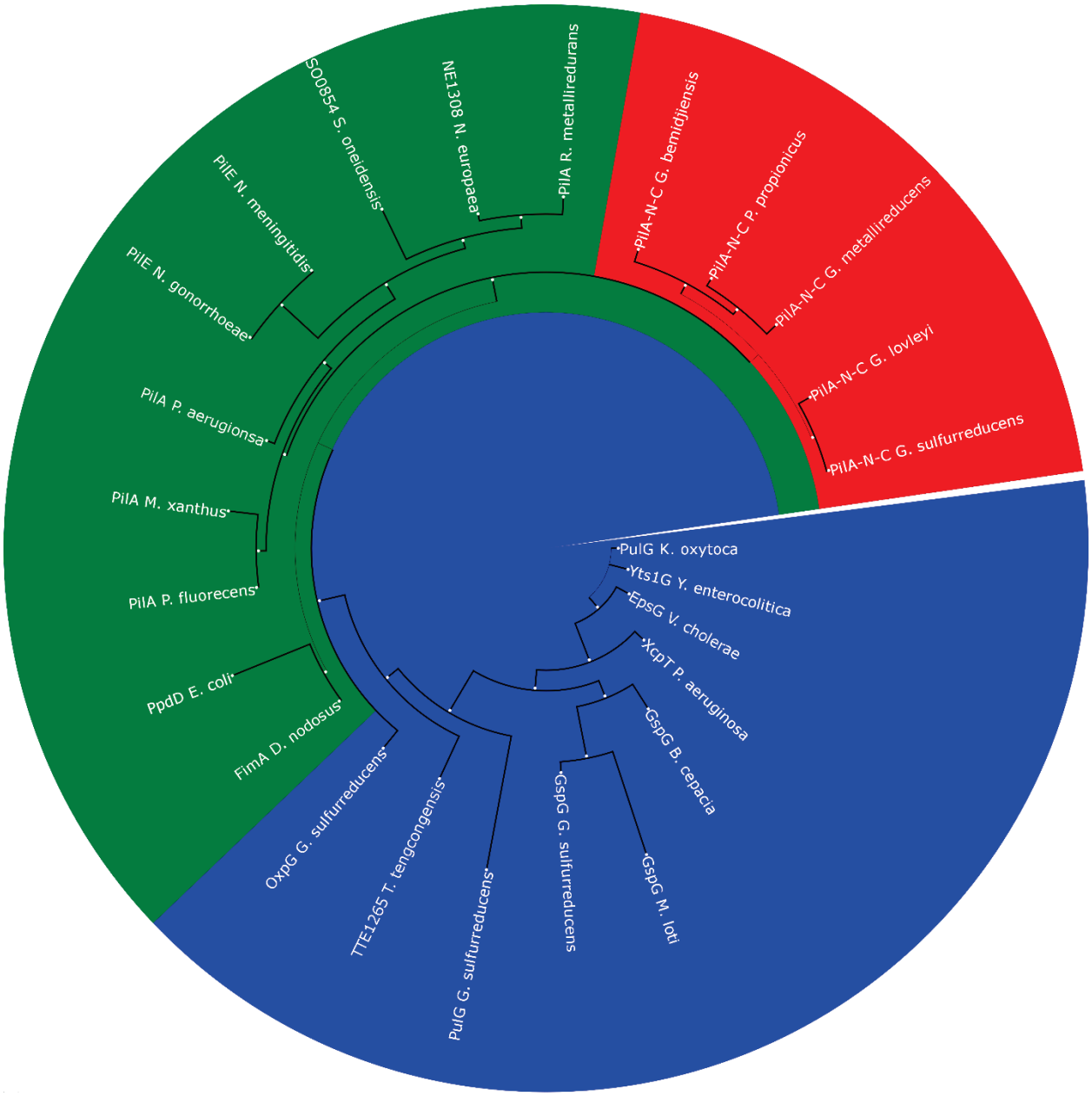

Supplementary Data Figure 1c. Rooted tree representation of the phylogenetic analysis of pilin amino acid sequence alignment of the T4P (blue) and T2SS pseudopili (blue) from different species. For *Geobacter*-related species, PilA-N and PilA-C sequences were fused together for comparison (shown in red).

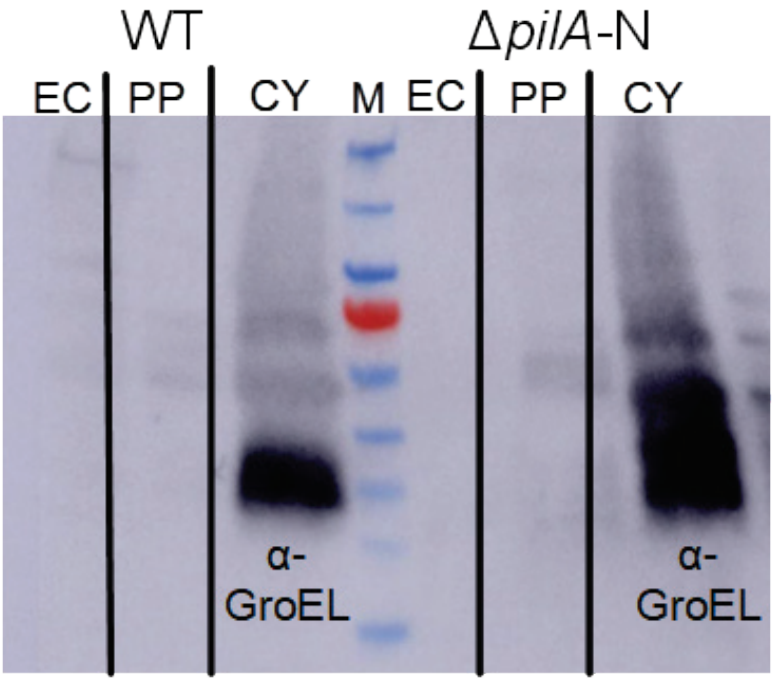

Supplementary Data Figure 2. Immunoblot showing control for subcellular fractionation studies using cytoplasmic protein GroEL. EC: Extracellular, PP: Periplasmic and CY: Cytoplasmic fractions. M:Marker.

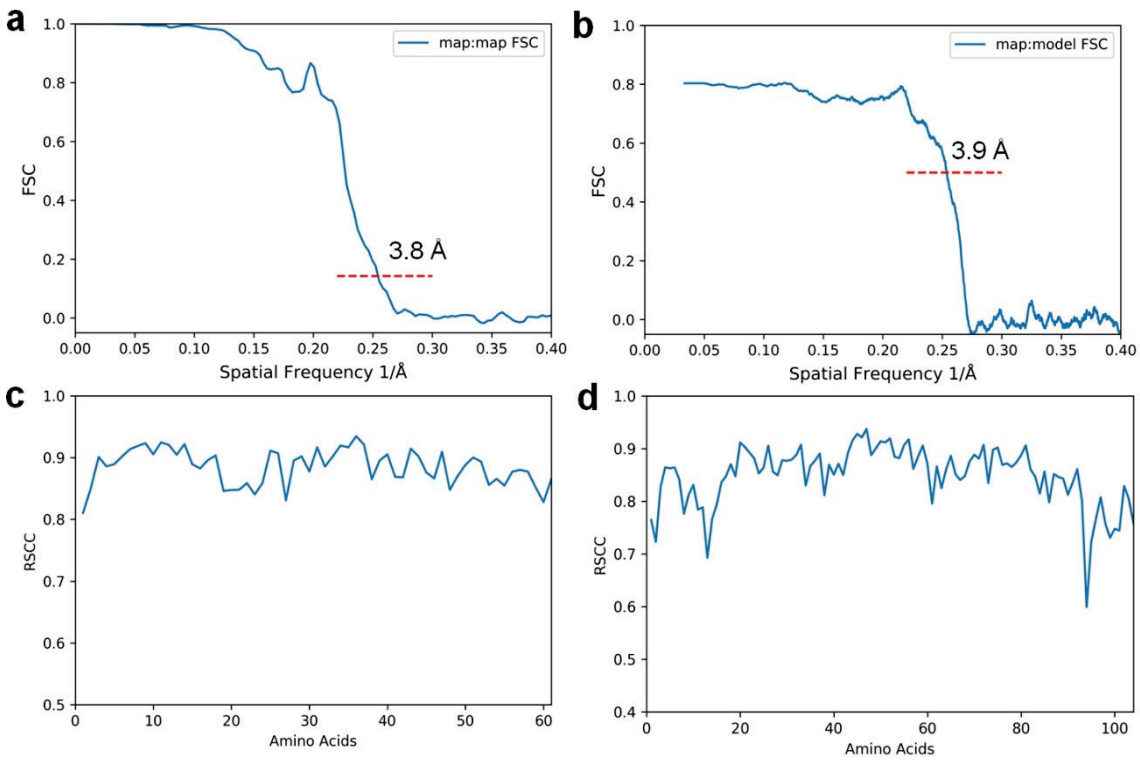

Supplementary Data Figure 3. Illustration of cryo-EM map quality. a, The gold standard FSC calculated by Relion using 0.143 cutoff estimated the map to have a resolution at 3.8 Å. **b,** Map to model FSC using 0.5 criterion estimated the map resolution to be 3.9 Å. **c,** The per-residue real space correlation coefficient plot of the atomic model against the map for PilA-N. **d,** The per-residue real space correlation coefficient plot of the atomic model against the map for PilA-C.

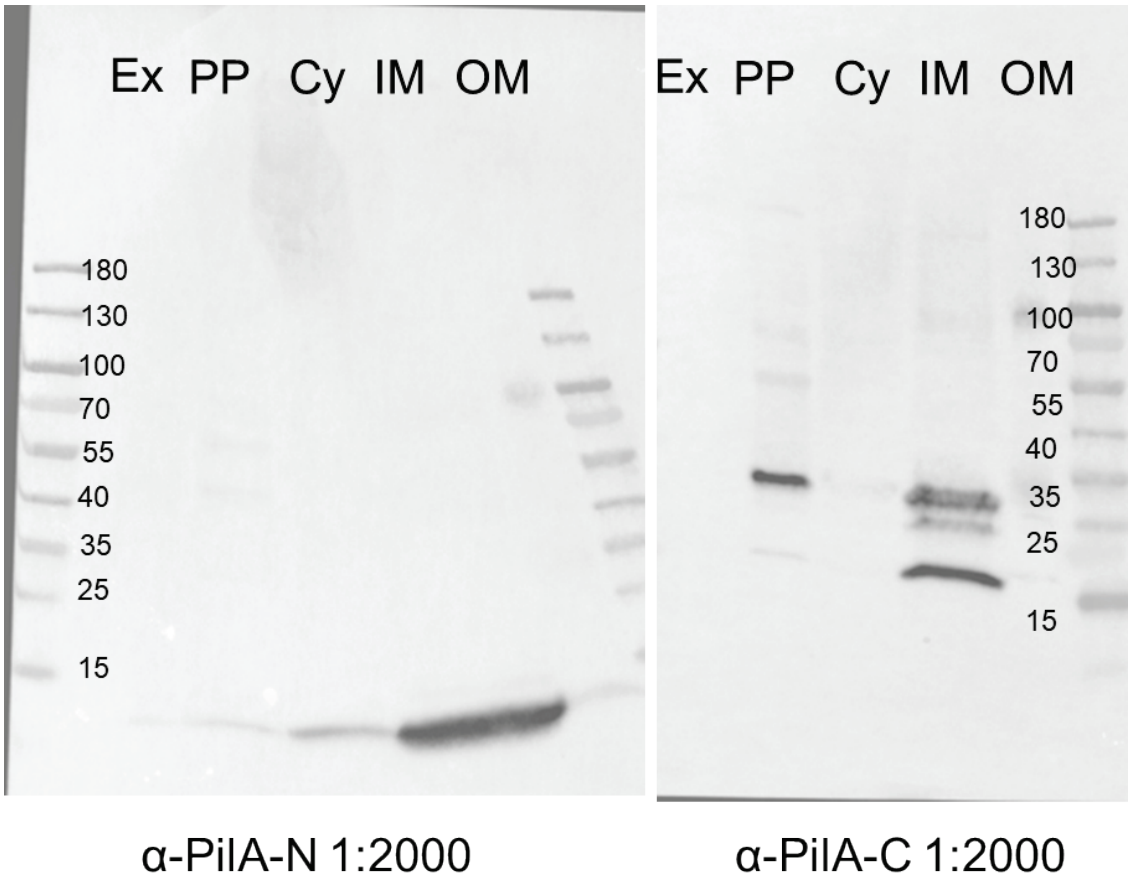

Supplementary Data Figure 4. Full-length gel showing lack of pili proteins in extracellular fractions. Immunoblot for subcellular fractionation of PilA-N and PilA-C in WT cells. Ex: extracellular, PP: Periplasm, CY: Cytoplasm, IM: Inner-membrane, OM: Outer-membrane

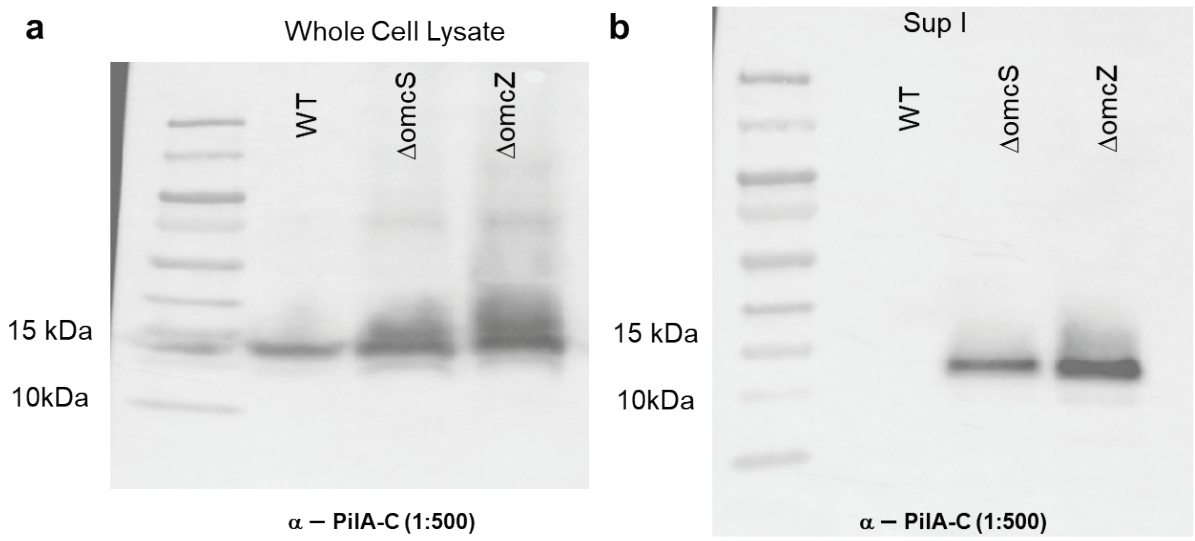

Supplementary Data Figure 5. Full-length gel showing overproduction of PilA-C in mutants lacking cytochrome nanowires. Immunoblot of PilA-C in WT, Δ*omcS* and Δ*omcZ* cells.

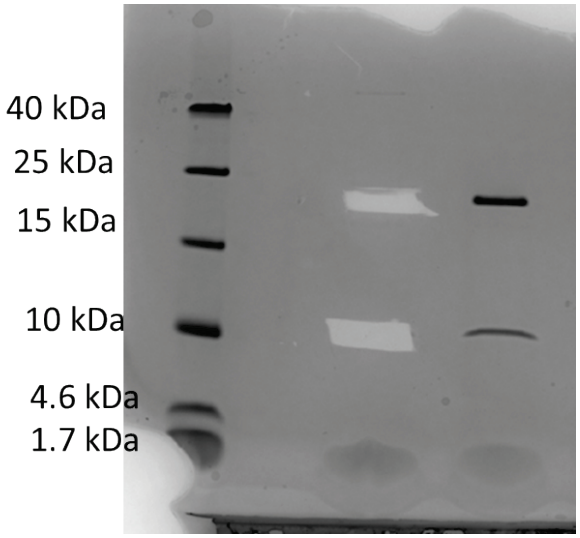

Supplementary Data Figure 6. Full-length SDS-PAGE gel of PilA-N-C filaments purified from Δ*omcS* cells.

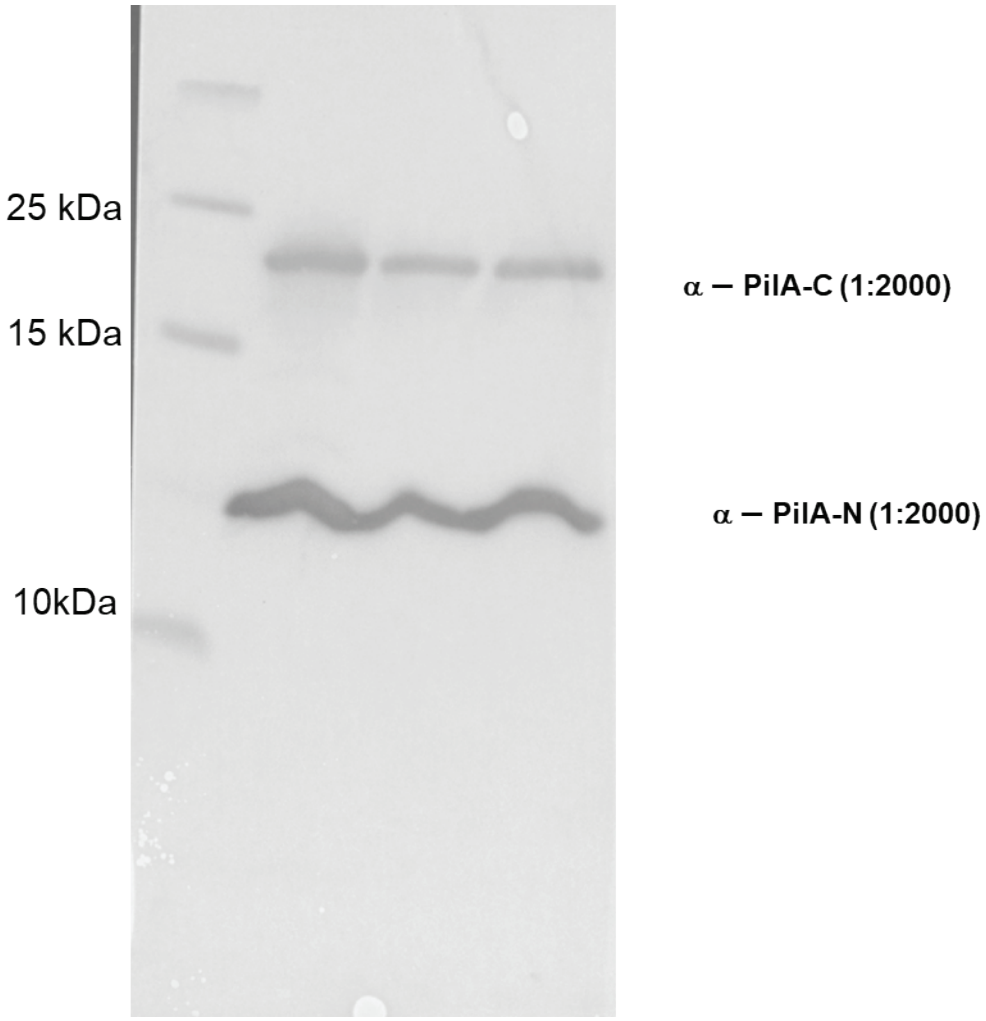

Supplementary Data Figure 7. Full-length immunoblot for PilA-N and PilA-C containing band.

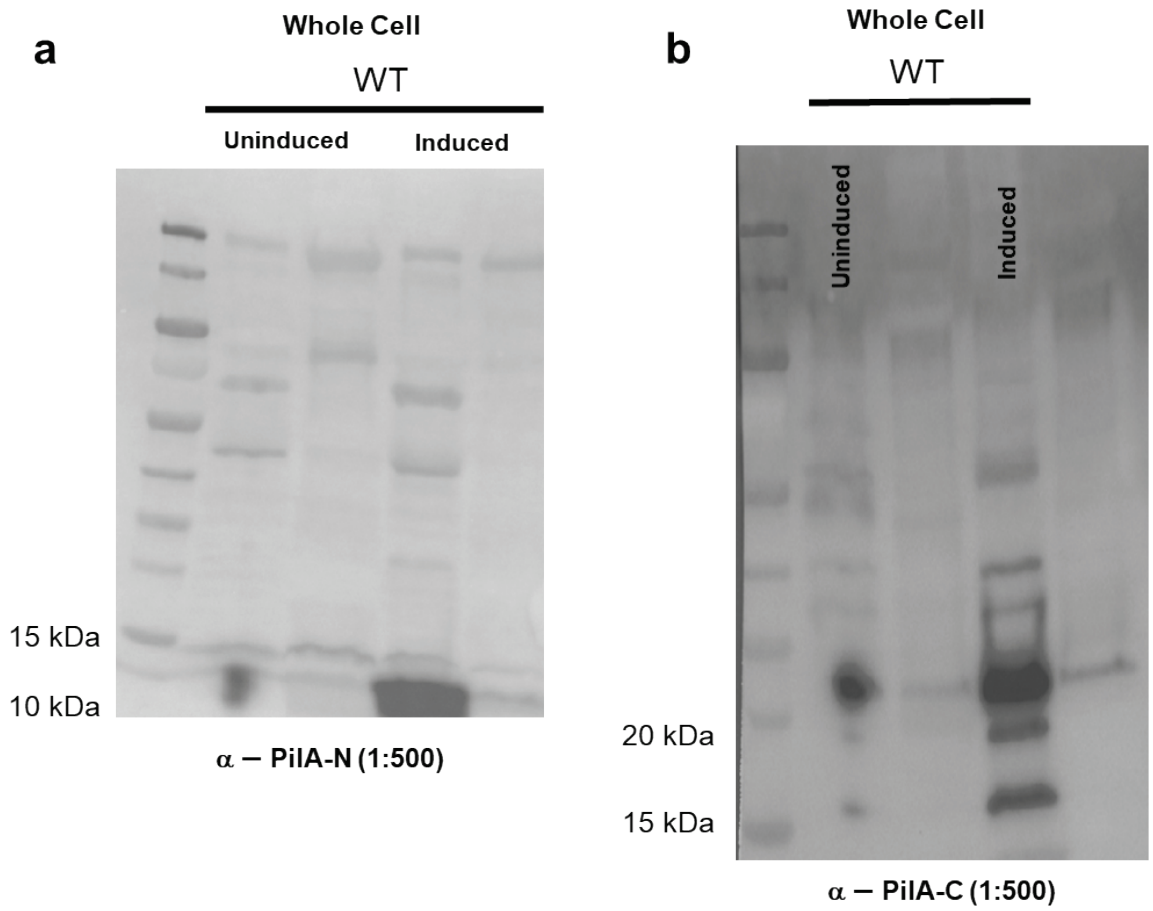

Supplementary Data Figure 8. Full-length immunoblot for overexpressing PilA-N and PilA-C in WT *G. sulfurreducens* yielded pili-like filaments. Immunoblot of whole cell lysate showing overexpression of **a,** PilA-N and **b,** PilA-C under induced conditions.

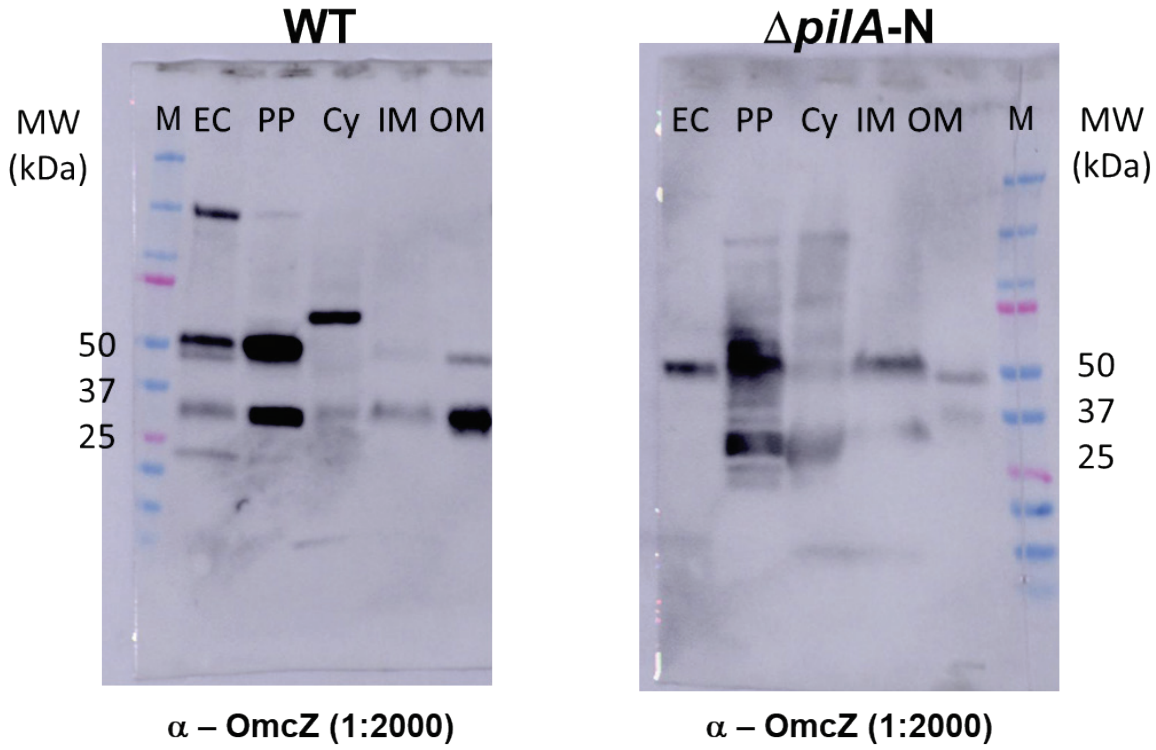

Supplementary Data Figure 9. Full-length gel showing lack of OmcZ nanowires in extracellular fractions of Δ*pilA*-N cells. Immunoblot for subcellular fractionation of OmcZ in WT cells and Δ*pilA*-N cells. EC: extracellular, PP: Periplasm, CY: Cytoplasm, IM: Inner-membrane, OM: Outer-membrane. M: Marker.

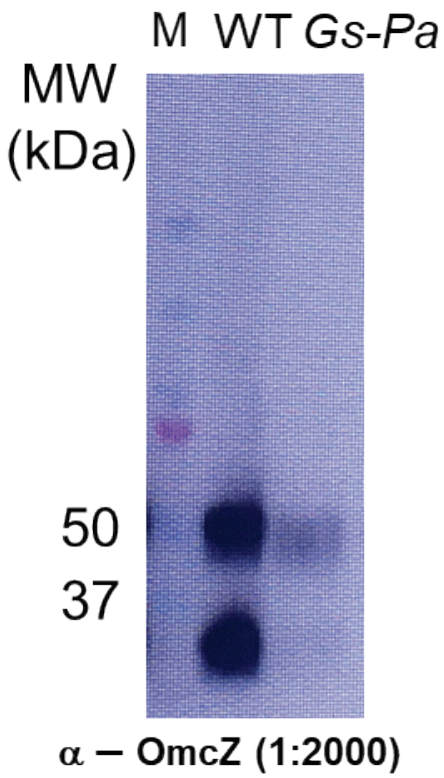

Supplementary Data Figure 10. Full-length gel showing lack of $OmcZ_S$ in filament preparations of *G. sulfurreducens* strains in which *pilA*-N was replaced with *pilA* of *P. aeruginosa* (*Gs-Pa*). M: Marker.

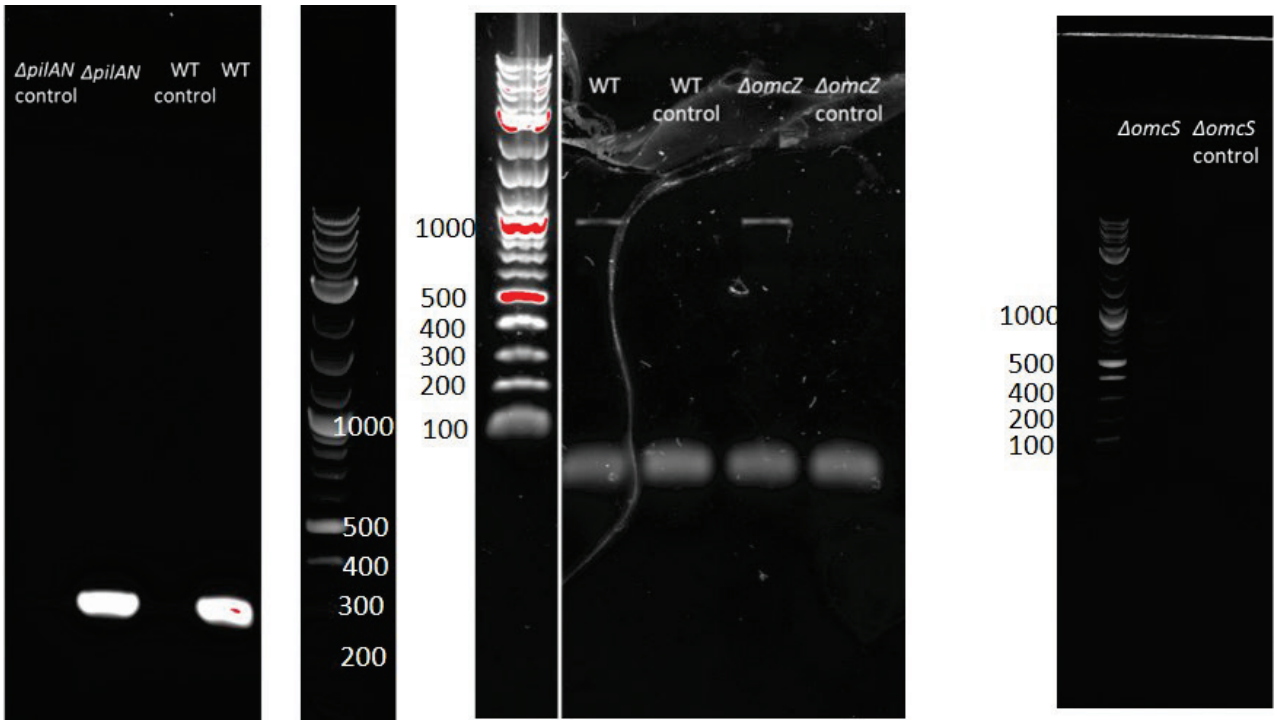

Supplementary Data Figure 11. Lack of polar mutations in Δ*pilA*, Δ*omcS* and Δ*omcZ* probed by RT-PCR using primers of downstream gene. Markers shows molecular weights in bp.

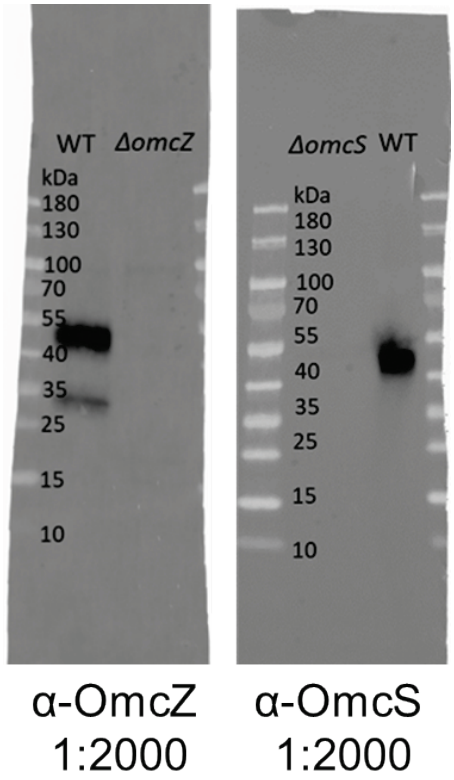

Supplementary Data Figure 12. Specificity of cytochrome antibodies using controls Δ*omcS* and Δ*omcZ*

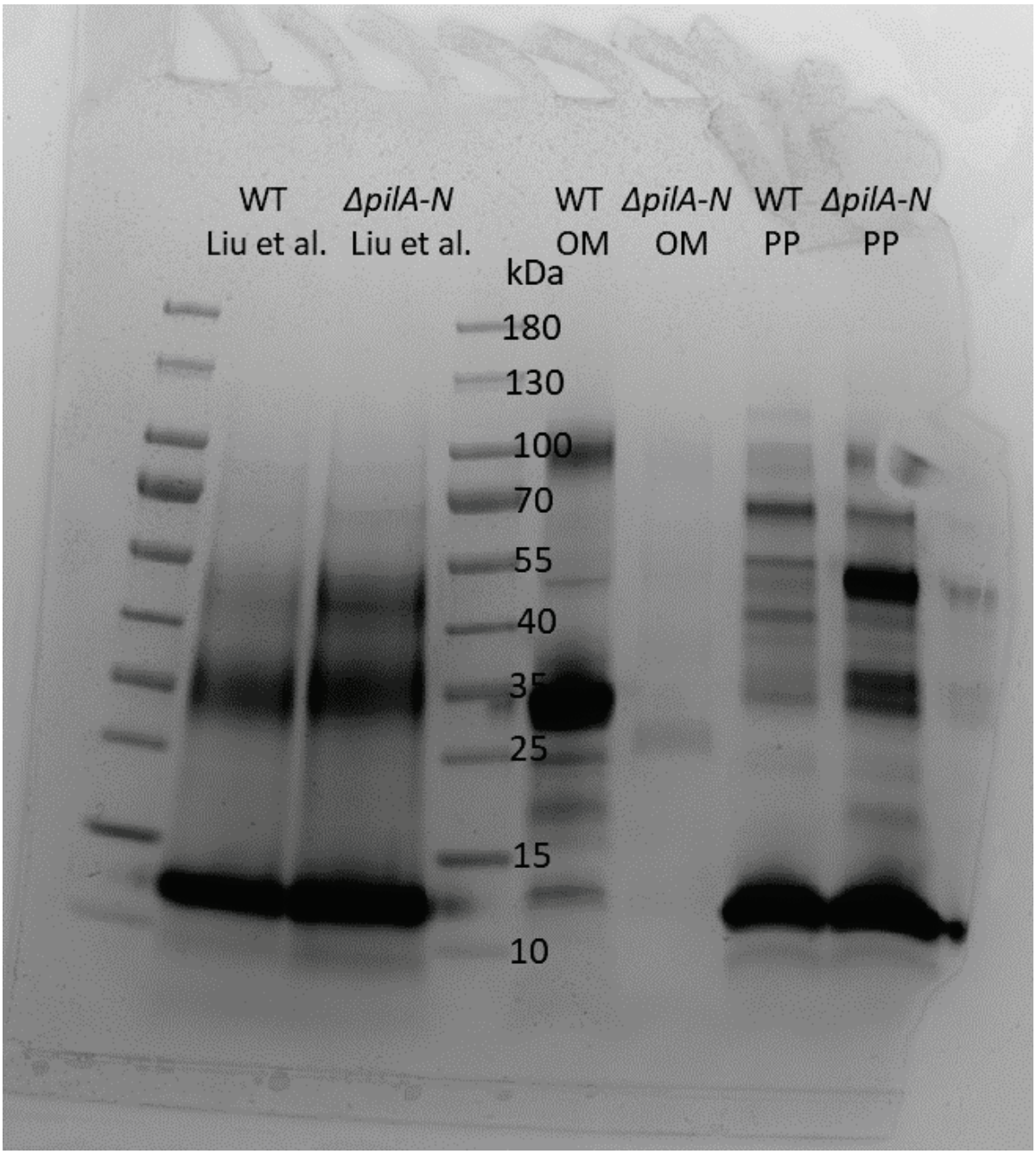

Supplementary Data Figure 13. Effect of periplasmic contamination in previous studies. Side-by-side comparison of extracellular cytochrome preparation protocol used by Liu et al. (Ref. 8) and the protocol used in this manuscript for outer-membrane (OM) and periplasmic (PP) fractions**.** The extracellular cytochrome preparation by Liu et al. seems to contain periplasmic contamination as evident by similarity with our periplasmic fractions.

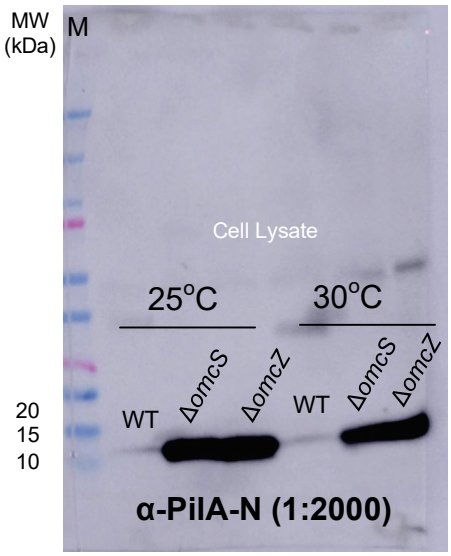

Supplementary Data Figure 14. Full-length gel of whole cell lysate showing overproduction of PilA-N in mutants lacking cytochrome nanowires. Immunoblot of PilA-N in WT, Δ*omcS* and Δ*omcZ* cells grown at 25ºC (left lanes) and 30ºC (right lanes)

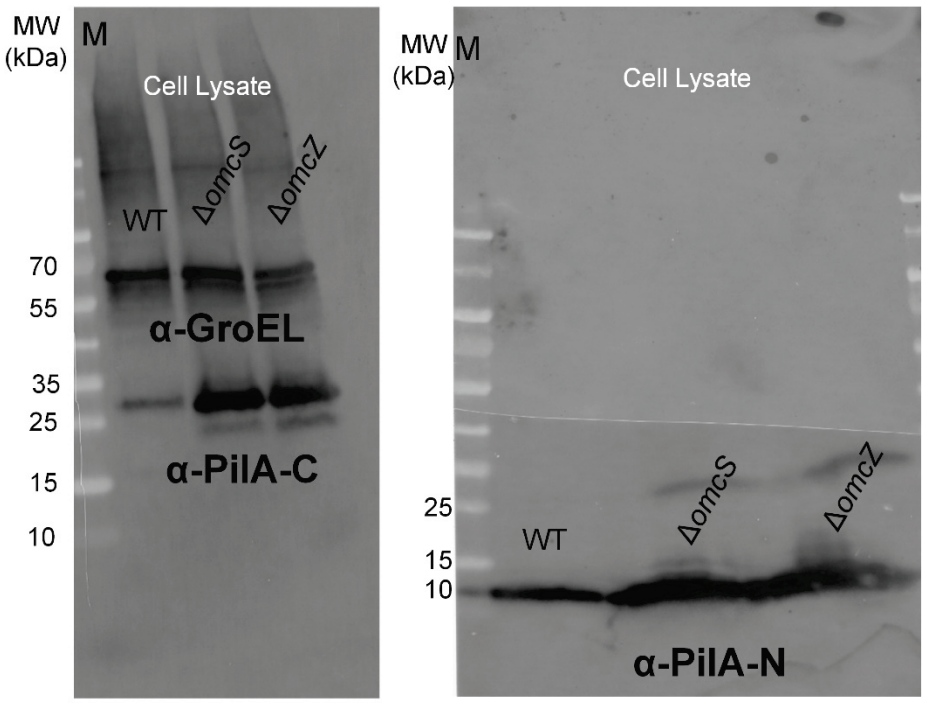

Supplementary Data Figure 15. Full-length gel of whole cell lysate showing overproduction of PilA-N and PilA-C in mutants lacking cytochrome nanowires. Immunoblot of GroEL, PilA-C and PilA-N in WT, Δ*omcS* and Δ*omcZ* cells. M: Marker

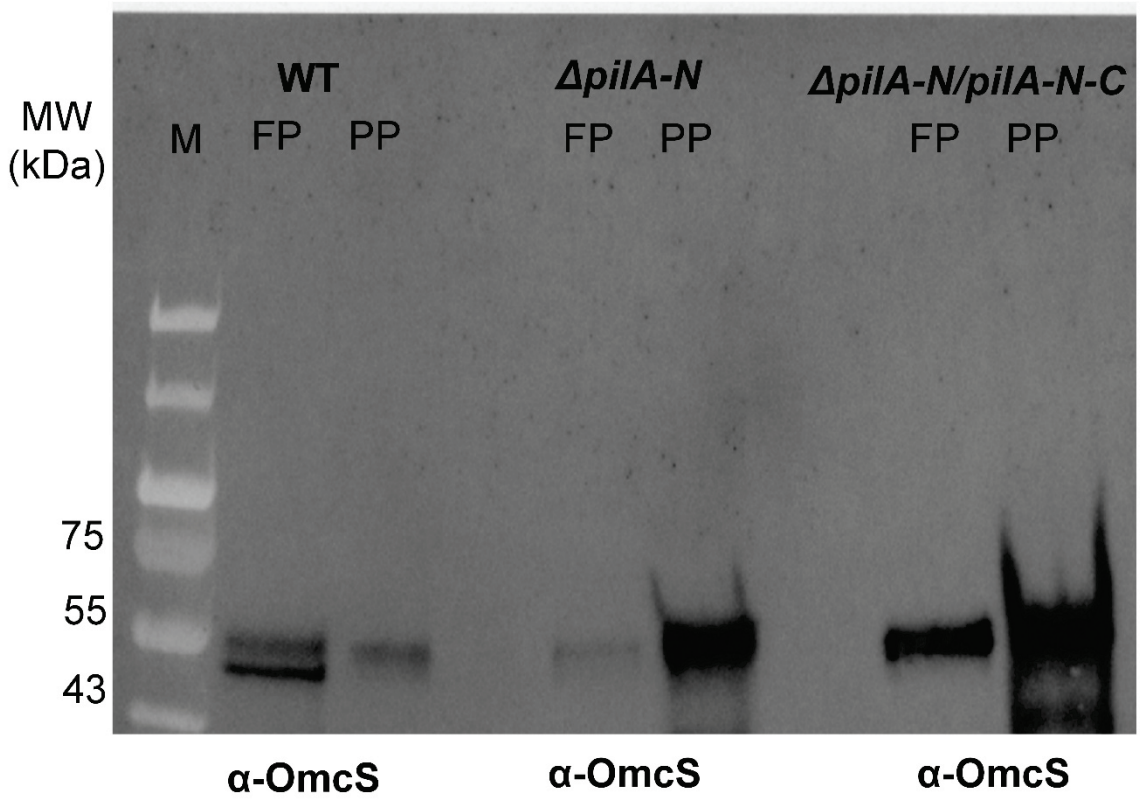

Supplementary Data Figure 16. Immuno-blotting with OmcS antibody showing the restoration of secretion defect in OmcS nanowires in *ΔpilA-N*/*pilA-N-C* cells. FP: Filament preparation. PP: Periplasmic fraction. M: Marker

Protein Name	MW (kDa)	Coverage(%)	iBAQ (x 10^8)
GSU3305	10	67	317
GSU3402	10	57	127
GSU0360	46	75	72.8
GroL	58	88	69.2
GSU3547	27	69	66.1
OmcZ	49	23	52.4
CpoB	31	71	44.2
Eno	46	78	40.1
PpcA	10	27	35.9
GSU0872	16	76	35.3
GlnA	53	86	32.4
DegP	50	81	31.3
GSU2429	39	74	29
GSU0800	29	63	28.1
OmcE	24	22	22.1
OmpB	140	58	21
OmcC	81	41	20.9
OmcB	77	19	7.8
OmcQ	36	16	0.24
OmcP	30	16	0.23
OmcS	45	25	0.17
OmcI	37	4	0.15

Supplementary Data Table 1. Lack of pili filaments under nanowire-producing conditions that required long-range electron transport. Solution mass spectrometry analysis of filament preparation from electrode-grown WT cells did not show either PilA-N or PilA-C.

	PilA-N-C filament (EMDB-21225) (PDB 6VK9)
Data collection and processing	
Magnification	165,000
Voltage (kV)	300
Electron exposure (e–/Å^2)	62
Defocus range (μm)	0.8 – 2.5
Pixel size (Å)	0.822
Symmetry imposed	89.1°/10.4 Å
Initial particle images (no.)	280000
Final particle images (no.)	100000
Map resolution (Å)	3.8
FSC threshold	0.143
Map resolution range (Å)	3.6 – 4.4
Refinement	
Initial model used (PDB code)	**6VK9**
Model resolution (Å)	3.9
FSC threshold	0.5
Model resolution range (Å)	
Map sharpening *B* factor (Å^2)	127
Model composition	
Non-hydrogen atoms	19792
Protein residues	2640
Ligands	NA
B factors (Å^2)	
Protein	NA
Ligand	NA
R.m.s. deviations	
Bond lengths (Å)	0.01 (0)
Bond angles (°)	1.699 (0)
Validation	
MolProbity score	1.91
Clashscore	7
Poor rotamers (%)	0.7
Ramachandran plot	
Favored (%)	90.06
Allowed (%)	9.64
Disallowed (%)	0

Supplementary Data Table 2. Cryo-EM data collection, refinement and validation statistics.

Stats	Input model	Refinement after Namdinator
Clash score	16.05	18.05
Favored	83.85%	80.82%
Ramachandran Outliers	0	0.3%
Rotamer Outliers	0	0.65%
CC value	0.84	0.86

Supplementary Data Table 3. Namdinator remodelling results. Namdinator remodelling did not improve the Ramachandran statistics.

Stats	Input model	Refinement after ISOLDE
Clash score	16.05	6.63
Favored	83.85%	90.06%
Ramachandran Outliers	0	0
Rotamer Outliers	0	0
CC value	0.84	0.84

Supplementary Data Table 4. ISOLDE remodelling results. ISODLE remodeling improved the statistics significantly.